ARPN Journal of Engineering and Applied Sciences

COLD FLOW BEHAVIOUR OF A SWIRLING FLUIDIZED BED INCINERATOR

Sulastri Sabudin, Wan Saiful-Islam Wan Salim and Mohd Faizal Mohideen Batcha
Energy Technologies Research Group, Centre for Energy and Industrial Environment Studies, Universiti Tun Hussein Onn Malaysia, Parit Raja, Batu Pahat, Johor, Malaysia
E-Mail: sulastri@uthm.edu.my

ABSTRACT

This paper reports the experimental work carried out to determine the cold flow behavior of a swirling fluidized bed incinerator (SFBI) with Quartz sand as bed particles. Three different sizes of sand particles were studied: 425-600μm, 600-850μmand 850-1180μm for four bed heights: 25 mm, 30 mm, 35 mm and 40 mm. The density of the particles was 2450 kg/m^{3}while the gas superficial velocity (U_s) was limited to 3 m/s. It was found that the larger particles exceeded the swirl-able regime and only possessed bubbling regime during fluidization. It was also found that the bed pressure drop was higher for higher bed heights and increased when the bed operates in the swirling regime. The study concludes that bed with the smallest particle size (425-600μm) and highest bed height (40 mm) has the desired characteristics to be used in the SFBI.

Keywords: cold flow behavior, swirling fluidized bed incinerator, pressure drop, minimum fluidization velocity.

INTRODUCTION

Fluidized bed technology is long known for its vast industrial applications such as thermal catalytic cracking of fuels, drying, combustion, gasification, particle heating and many other processes that involve solid-fluid contact. Fluidized beds are simply a bed of particles in which fluid flows through the bed and the drag force by the fluid is large enough to suspend the bed. This intimate contact between the bed and fluid provides huge potential for reaction to take place between the two, in comparison to its packed condition. Many variants of fluidized bed are available in the industry at present where each of them is usually designed for a specific application. Among these variants is one which operates based on swirling principle where swirling motion is created inside the bed to promote lateral mixing of the bed, increase gas residence time and reduce elutriation of finer particles. These types of bed are usually compact by having significant aspect ratio (diameter to height).In general, swirling may be achieved by several ways such as secondary injection into the freeboard using nozzles or using a distributor which provides inclined injection of air to the bed. The latter approach has recently gained interest among researchers particularly in combustion studies. However, before a thermal system is developed for industrial use, its cold flow behaviour must be determined first to estimate the system's resistance which later translates into operational costs. In the case of a fluidized bed system, it's cold flow behaviour includes the distributor pressure drop (Δp_d), bed pressure drop (Δp_b), minimum fluidization velocity (U_{mf}) and regimes of operation.

Kaewklum *et al.,* 2009, have studied the hydrodynamic regimes and characteristics of a conical swirling fluidized bed for Quartz sand of four different sizes and compared the effect of tangential and axial entries into the bed. They have also investigated the effect of various bed heights and proposed a mathematical model to predict minimum fluidization velocity (U_{mf}) and bed pressure drop (Δp_b). They reported that the bed exhibits four distinct regimes of operation, namely fixed-bed, partially fluidized-bed, fully fluidized-bed with partial swirling and fully swirling fluidized-bed. They concluded that both air entry types influenced the bed's hydrodynamics significantly and they opted the axial entry bed with annular-blade distributor for their following studies on biomass combustion (Kaewklum and Kuprianov, 2010).

Much earlier, prediction of minimum fluidization velocity and particle trajectory was done by Shu *et al.,* 2000 through a minor modification of existing mathematical models available in the literature. Geldart type A and type C particles were used during experiments in a pilot scale Torbed® reactor. A similar effort was later reported by Sreenivasan and Raghavan, 2002 for large particles (Geldart type-D) in which the authors highlighted their important finding – the increase of bed pressure drop with increasing superficial velocity in swirling mode due to the centrifugal bed weight. An approximate model for predicting the bed's angular velocity was also proposed by the authors for shallow bed heights by assuming the bed as a lumped system.

The hydrodynamic characterization and heat transfer studies in the swirling bed was also reported by Mohideen *et al.,* 2012a for extra-large particle sizes (5 mm to 10 mm) for deeper beds.The authors reported the presence of secondary motion of the bed in atoroidal path and highlighted the potential of the bed in biomass processing. Hydrodynamic and drying experiments of oil palm frond (OPF) biomass by Mohideen *et al.,* 2011 confirms this, and the authors highlighted the rapid moisture removal from both leaves and stem (petiole). Based on the hydrodynamics and drying kinetics of OPF, the authors concluded the swirling fluidization is a viable technique for drying of OPF despite its irregular shape and density variation.

ARPN Journal of Engineering and Applied Sciences

Recently, Zakaria *et al.,* 2014 reported the success of drying pliant media using a swirling fluidized bed dryer. In their study, the pliant media dried was an industrial grade sponge which at present is widely used for surface preparation in oil and gas industry. The wet sponge particles were dried at U_{mf} to reduce energy loss due to bed pressure drop. This was because in a typical swirling bed, Δp_b increases with increasing U_s due to the centrifugal bed weight. The vigorous mixing of the pliant media allows quick drying without the re-wetting problem that usually occurs in hygroscopic material such as the sponge.

In this study, experimental work were carried out to determine the cold flow behavior of a swirling fluidized bed incinerator (SFBI) with Quartz sand as bed particles. Three different sizes of sand particles were studied: 425-600µm, 600-850µm and 850-1180µm for four bed heights: 25 mm, 30 mm, 35 mm and 40 mm. The findings of this study were imperative to develop a SFBI which is capable in incinerating various types of waste efficiently.

MATERIALS AND METHOD

Swirling Fluidized Bed Incinerator (SFBI)

The SFBI in this study uses an annular-blade type distributor, similar to the previous researchers (Shu *et al,* 2000), (Sreenivasan and Raghavan, 2002) and (Mohideen *et al.,* 2012a). The plenum chamber provides the air tangentially to the base of the bed while the acrylic column provides good visibility of the bed for characterizing the bed operating regimes. Figure-1 shows the overall SFBI system with auxiliary equipment while Figure-2 depicts the details of the experimental set-up used for the old flow study.

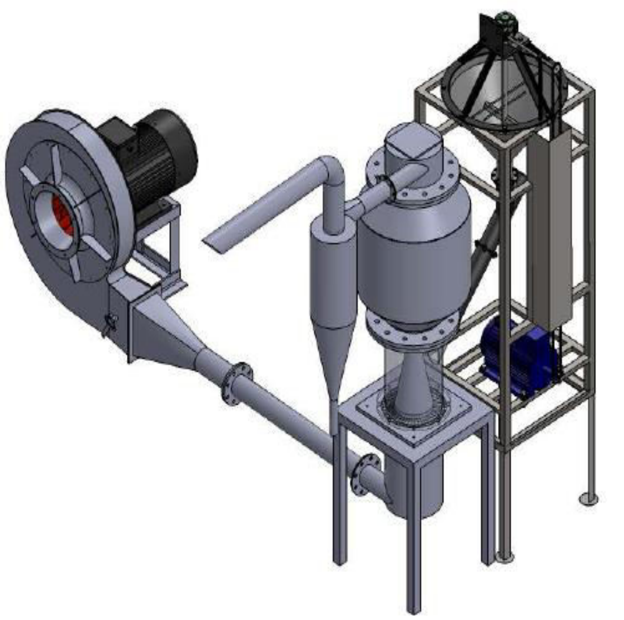

Figure-1. The swirling fluidized bed incinerator (SFBI) system with auxiliary equipment.

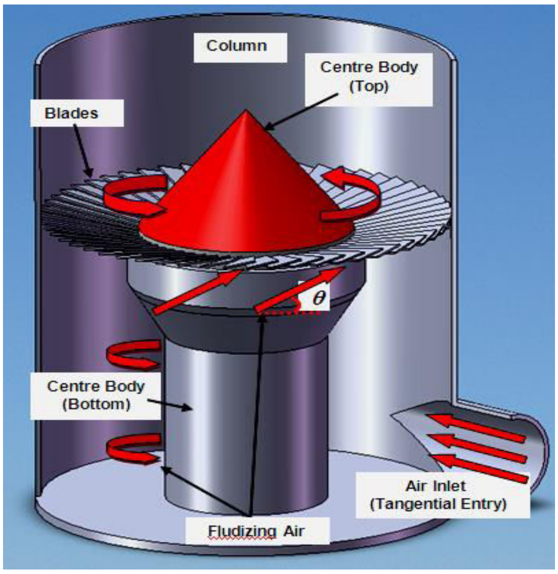

Figure-2. SFBI detailed design.

Referring to Figure-2, air enters the SFBI tangentially at the bottom (plenum chamber) before flowing upwards in a swirling motion towards the distributor. Owing to the inclination of the distributor blades at the angle θ and due to the small opening between the blades, the air now jets from the distributor (at the angle θ) and possesses both horizontal and vertical momentum. The horizontal momentum swirls the bed while the vertical momentum fluidizes the bed. The center body on top of the distributor avoids dead zone and creates an annular region for incineration to take place.

Sample preparation

The Quartz sand in this study was first sieved to three size ranges: 425-600µm, 600-850µm and 850-1180µm. Water displacement method was used to determine the volume of knowns and mass and the density was found to be 2450 kg/m^3.This value and the average particle sizes were then used to classify the sand based on Geldart's diagram for powder classification, which is reproduced from Howard, 1989 as in Figure-3.

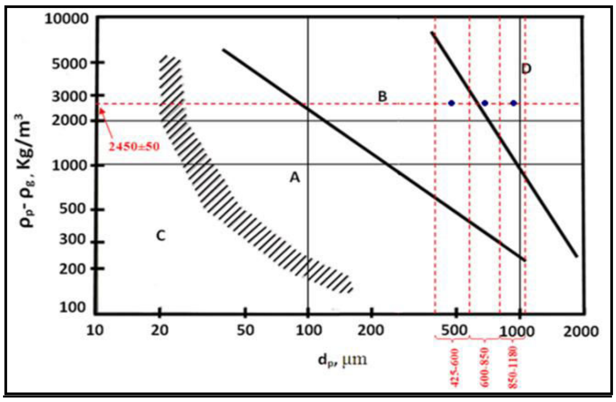

Figure-3. Geldart's classification for powders (Howard, 1989).

VOL. 11, NO. 18, SEPTEMBER 2016 ISSN 1819-6608
ARPN Journal of Engineering and Applied Sciences

Experimental procedure

Sand of a given size was poured into the bed from top. The bed was then fluidized vigorously before the fluidizing air velocity was gradually reduced. The bed height was measured at three different locations using pre-attached scale on the bed column. Additional sand was poured (if necessary) until the bed reached the required height. Air was introduced to the bed gradually while the bed pressure drop was measured (between distributor and top of the bed). The Δp_b values were recorded and the bed behaviour was observed closely to establish the regimes of operation. The supply air was limited to 3 m/s since this velocity was found to be appropriate in the present study from preliminary experiments. Upon recording the U_s and Δp_b values, experiments were repeated for the other bed heights: 30 mm, 35mm and 40 mm and other sand particle sizes. In the present study, the velocity was measured using a pitot-static probe just before the plenum chamber inlet while the Δp_b values were measured using a digital-micro-manometer. Upon completion of experiments with particles, the bed was emptied and the distributor pressure drop, Δp_d was recorded with increasing U_s.

RESULTS AND DISCUSSIONS

Distributor pressure drop against velocity

As shown in Figure-2, the distributor in this study was made by an array of truncated annular blades with a centre body (cone) in the middle. These blades were inclined 15º to the horizontal plane to provide inclined injection of air into the bed. The total number of blades was 45 which correspond to a fraction of open area (FOA) of 15%. This relatively large FOA yields a low distributor pressure drop, Δp_d without compromising the fluidization quality (Shu *et al.,* 2000 and Sreenivasan and Raghavan, 2002). Figure-4 shows the Δp_d against U_s in the present study.

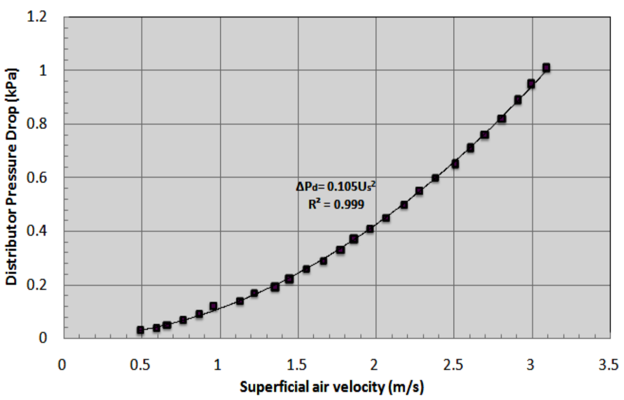

Figure-4. Δp_d against U_s for annular blade distributor in the SFBI.

Besides being one of the hydrodynamic characteristics, the Δp_d also enables the determination of its individual contribution to the overall system resistance. Lower Δp_d is always preferred but without any adverse effect on the fluidization quality. The Δp_dhere may be attributed to the abrupt contraction of the process gas at the inlet of the distributor, flow of the process gas through the opening of the distributor blades and sudden expansion at the distributor outlet. Based on linear regression analysis, the Δp_d can be correlated with U_s by the equation: $\Delta p_d = 0.105U_s^2$with a correlation coefficient (R^2) of 0.999, which indicates a second-order polynomial relation between both parameters.

Regimes of operation

The typical regimes of operation in a bubbling fluidized bed are packed bed, minimum fluidization, bubbling, slugging and finally elutriation. In the SFBI however, the regimes of operation were found to differ due to the swirling motion of the bed. Typical regimes of operation in the SFBI were shown in Figure 5 by taking the600-850μm sand particles with 30 mm bed height as an example.

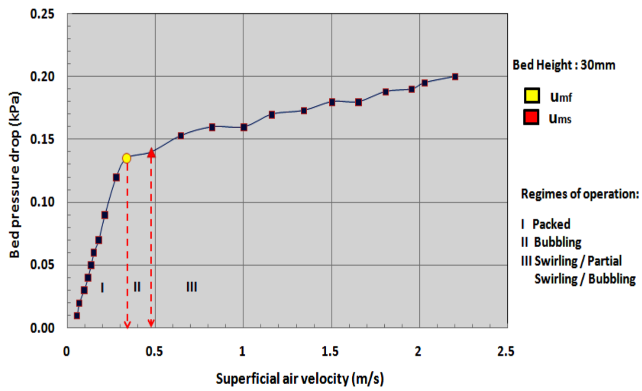

Figure-5. Typical regimes of operation in the SFBI (600-850μm particles, bed height: 30 mm)

Referring to Figure-5, the bed was initially in packed condition whereby the U_s is insufficient toprovide enough drag force to suspend the bed. The bed remained in the same condition until random bubbles started to appear on the bed surface with further increase of superficial velocity, U_s. Now the bed expands to allow more air to flow through the bed and bubbles were seen on the surface of bed. The Δp_b increased with U_s linearly in this region. Further increase of U_s results in more expansion of the bed until it reached the minimum fluidization, U_{mf} where the whole bed was suspended and balanced by the drag force. From U_{mf}, a slight increase in U_s resulted in the bed achieving minimum swirling condition denoted as U_{ms} in Figure-5. At U_{ms}, the bed was seen to gently swirl and further increase of U_s resulted in faster swirling of the bed. This was true for all bed heights. On the other hand, different regimes were observed for 600-850μm and 850-1180μm bed. For 600-850μm, the bed only swirls for 25 mm bed height and partially swirl for 30 mm bed height. Deeper beds were subjected to bubbling regime only. As for the 850-1180μm bed, the bed only possess bubbling regime for the whole range of bed height indicating the particle size has exceeded the

VOL. 11, NO. 18, SEPTEMBER 2016 ISSN 1819-6608
ARPN Journal of Engineering and Applied Sciences

www.arpnjournals.com

swirl-able regime in the present bed configuration. These findings are summarized in Table-1 below:

Table-1. Operational regime in the SFBI.

Sand particle size (µm)	Bed Height			
	25mm	30mm	35mm	40mm
425-600	//	//	//	///
600-850	//	/	--	--
850-1180	--	--	--	--

Legend	Observation Rating
///	Excellent Swirling
//	Good Swirling
/	Bubble or partial swirl
--	Bubbling

Effect of bed height

In this study, the three particles studied were from different categories of Geldart's classification. While the425-600µm and 850-1180µm particles were from Geldart type B and D, the 600-850µm particles were near the transition region between B and D. The behaviour of these particles was presented in Figures 6 to 8:

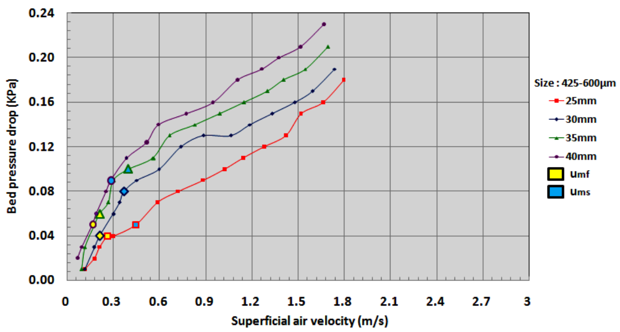

Figure-6. Δp_b against U_s for 425-600µm particles.

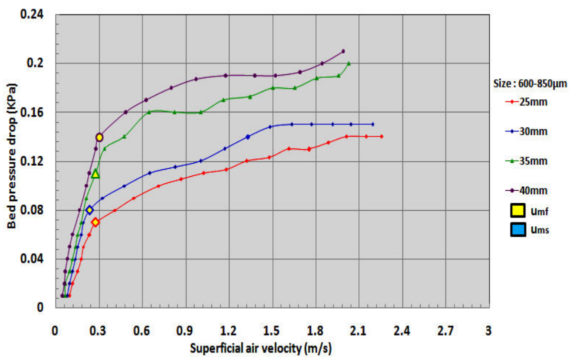

Figure-7. Δp_b against U_s for 600-850µm particles.

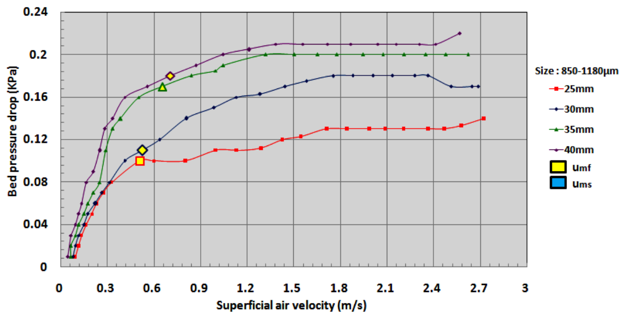

Figure-8. Δp_b against U_s for 850-1180µm particles.

In general, higher bed heights have larger Δp_b due to the larger bed mass acting on the given distributor area. Therefore, larger drag force was required to initiate both fluidization (as well as swirling) in the bed. In the packed region, the gradient of $\left[\frac{d(\Delta p_b)}{d(\Delta U_s)}\right]_{packed}$ was found to be constant indicating the linear increase of Δp_b with U_s. However, the 425-600µm particles showed a distinct characteristic in which the Δp_b increased significantly beyond $U_{mf}$with a linear trend. The $\frac{d(\Delta p_b)}{d(\Delta U_s)}$ however, was less than that of the packed region. The significant increase of Δp_bcan be explained by the increasing centrifugal bed weight as a result of increased angular momentum at higher U_s. Apart from that, the smaller particles sizes possess larger surface area for a given bed loading, thus translates to higher Δp_b due to augmented inter-particle friction apart from friction with distributor as well as the column wall.

In Figure-7 and 8, beyond U_{mf}, the $\frac{d(\Delta p_b)}{d(\Delta U_s)}$ for 600-850µm and 850-1180µm particles were relatively smaller than that for 425-600µm (Figure 6) due to the absence of swirling motion for all bed configurations (except for the 25 mm bed height for 600-850µm particles). It was also seen that the U_{mf} values for a given particle size were has a small difference for a given bed height. These U_{mf} values were summarized in Table-2.

Table-2. Summary of U_{mf} values for a given bed height.

Sand particle size (µm)	Bed height (mm)	U_{mf} (m/s)
425-600	25	0.20
	30	0.18
	35	0.18
	40	0.19
600-850	25	0.27
	30	0.25
	35	0.25
	40	0.30
850-1180	25	0.53
	30	0.54
	35	0.66
	40	0.69

ISSN 1819-6608
ARPN Journal of Engineering and Applied Sciences

www.arpnjournals.com

Effect of particle size

The effect of various particle sizes for a given bed height were presented in Figures-9 to 12. It could be seen that the operating velocity range for 425-600µm particles was limited to about 1.8 m/s due to elutriation of fines from the bed during experiments.

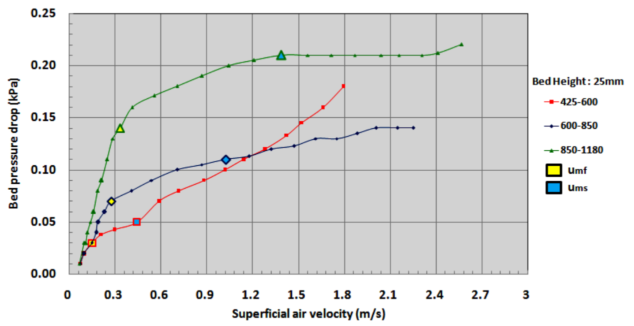

Figure-9. Δp_b against U_s for bed height = 25 mm.

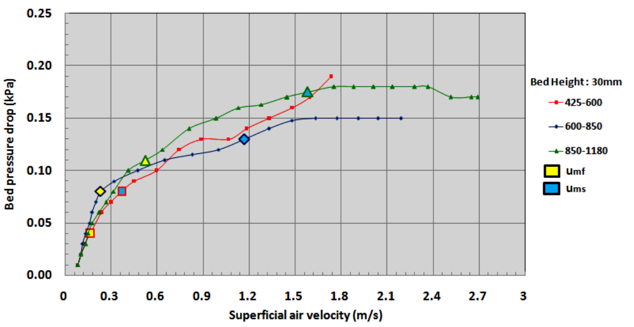

Figure-10. Δp_b against U_s for bed height = 30 mm.

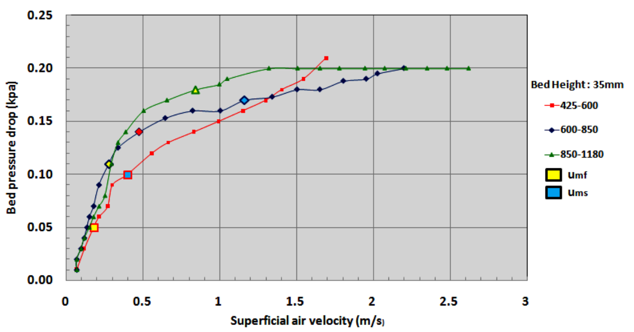

Figure-11. Δp_b against U_s for bed height = 35 mm.

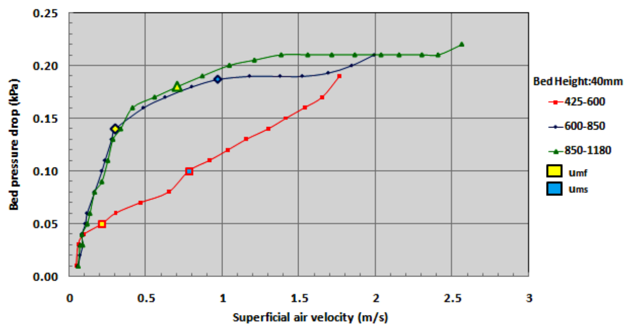

Figure-12. Δp_b against U_s for bed height = 40 mm.

Typically the Δp_b against U_s for smaller particles were slightly larger in the packed region due to the higher surface area of the particles. From Figure-9, 10 and 11 (25, 30 and 35 mm bed height), the Δp_b was found to be much higher for larger particles in the initial stages of fluidization.

Apparently, with continuous increase of U_s, the Δp_b of 425-600µm particles surpasses the Δp_b of the other two particles. This may be explained by the regimes of operation undergone by each particle as addressed in the earlier in part of this paper. The two larger particles were experiencing bubbling regime and hence the Δp_b becomes constant with higher U_s beyond U_{mf}. In contrast, the 425-600µm particles swirl vigorously and the centrifugal force of the bed resulted higher frictional force at the bed wall and hence increased the Δp_b. This effect however was not visible in Figure-12 due to the limited operating velocity of the 425-600µm particles and significantly higher amount of bed weight for this bed height

CONCLUSIONS

From the cold flow study carried out in the SFBI, it can be concluded that both particle size and bed height influences the bed behaviour, particularly its operating regimes. The 425-600µm particles were able to swirl vigorously for all bed heights while the 600-850µm particles were capable to swirl only for shallow bed height (25 mm). The 850-1180µm was found to only possess bubbling regimes for all bed heights studied. Due to the swirling of the 425-600µm particles, its Δp_b increased with increasing U_s and the particles have limited operating Us range up to 1.8 m/s only. From the study, it may concluded that the 425-600µm particles with 40 mm bed height was advantageous to be used in the SFBI due to the excellent swirling nature of the bed as well as having the largest surface area for heat transfer during incineration.

REFERENCES

[1] Kaewklum, R., Kuprianov, V.I. and Douglas, P.L. (2009). Hydrodynamics of air–sand flow in a conical swirling fluidized bed: A comparative study between tangential and axial air entries, Energy Conversion and Management, 50, pp. 2999–3006.

[2] Kaewklum, R. and Kuprianov, V.I. (2010). Experimental studies on a novel swirling fluidized-bed combustor using an annular spiral air distributor, Fuel, 89, pp. 43-52.

[3] Shu, J., Lakshmanan V.I. and Dodson, C.E. (2000). Hydrodynamic study of a toroidal fluidized bed reactor, Chemical Engineering and Processing,39, pp. 499-506.

[4] Sreenivasan, B., and Raghavan, V. R. (2002). Hydrodynamics of a swirling fluidised bed. Chemical Engineering and Processing: Process Intensification,41(2), 99-106.

[5] Mohideen, M.F., Seri, S.M. and Raghavan, V.R. (2012a), Fluidization of Geldart type- D particles in a Swirling Fluidized Bed, Applied Mechanics and Materials, 110-116, pp. 3720-3727.

[6] Mohideen, M.F., Sreenivasan, B., Sulaiman, S.A. and Raghavan, V.R. (2012b). Heat transfer in a swirling fluidized bed with Geldart type-D particles, Korean J. Chem. Eng., 29 (7), pp. 862-867.

[7] Mohideen, M. F., Faiz, M., Salleh, H., Zakaria, H. and Raghavan, V. R. (2011). Drying of oil palm frond via swirling fluidization technique. In Proceedings of the World Congress on Engineering, 3, pp. 2375-2380.

[8] Zakaria, J. H., Zaid, M., Hashemi, M. H., Mohideen Batcha, M. F., & Asmuin, N. (2014). Drying of sponge media using swirling fluidized bed dryer. Applied Mechanics and Materials, 660, 644-648.

[9] Batcha, M. F. M., Nawi, M. A. H. M., Sulaiman, S. A., and Raghavan, V. R. (2013). Numerical Investigation of Airflow in a Swirling Fluidized Bed. Asian Journal of Scientific Research, 6(2), 157-166.

[10] J.R Howard (1989). Fluidized Bed Technology: principle and applications. Adam Hilger Imprint by IOP Publishing Ltd.